VARIABLE VISCOSITY AND CHEMICAL REACTION EFFECTS ON MHD FLOW OF RADIATIVE FLUID PAST A STRETCHING SHEET IN THE PRESENCE OF JOULE HEATING

Abstract

The focus of the present study is to examine chemical reaction and Joule heating effects on steady flow of a viscous radiating fluid in a porous medium under the influence of variable viscosity. The fluid viscosity is assumed to vary exponentially with temperature. The governing equations of flow, heat and mass transfer are transformed into ordinary differential equations using appropriate similarity transformations. The converted ordinary differential equations are then solved numerically by using fourth order Runge-Kutta Fehlberg method. The effects of different pertinent parameters on the flow, heat and mass transfer characteristic are analyzed and discussed in detail through graphs and table. It is observed that larger values of variable viscosity parameter depreciates the fluid velocity.

Keywords
Magnetohydrodynamic, Joule Heating, Temperature Dependent Viscosity, Porous Medium, Radiation.

1 Introduction

Magnetohydrodynamics (MHD) is a branch of fluid dynamics which studies the behavior of an electrically-conducting fluid in motion. Various areas of application of MHD fluid flow include electrostatic filters, purification of crude oil, MHD pumps, cooling reactors, MHD power generation etc. Ryoichi et al. [1] studied the application of MHD to flow of an electrolyte in an electrode-cell with short rectangular channel. Pakmor et al. [2] discussed numerical solutions of moving-mesh code in the presence of applied magnetic field. The combination of Lagrangian and Eularian methods was used in a single computation technique. Opanuga et al. [3] used Adomian decomposition method to solve the problem of Joule heating effects on MHD flow of reactive viscous fluid in a porous medium. Gedik et al. [4] numerically investigated MHD pressure induced flow through a pipe in the absence of slip conditions. A numerical simulation based on the finite volume method was employed by Azimi-Boulali et al. [5] to investigate a 3D model of Newtonian magnetohydrodynamic fluid flow. Zaman et al. [6] presented the exact solution of unsteady MHD fluid flow in a channel under the influence of heat transfer and slip conditions.

The study of heat transfer effect on fluid flow is of great importance in engineering and industry. A vast number of researchers have investigated heat transfer and boundary layer flow in the presence of several fluid properties. Rao et al. [7] studied the feature of MHD flow and convective heat transfer of nanofluid with chemical reaction effect. Mendal et al. [8] discussed

the effects of mass diffusion and thermal radiation on laminar unsteady free convective fluid flow in a vertical channel. Miroshnichenko and Sheremet [9] investigated the unsteady free convection flow of viscous fluid in the presence of heat transfer. Samuel [10] presented analytical solutions of chemical reaction and melting heat transfer effects on steady incompressible MHD Newtonian fluid flow in the presence of buoyancy force. Saravanan and Chinnasamy [11] studied the impacts of heat transfer on buoyancy driven flow of a viscous incompressible fluid under the influence of thermal radiation. Satya et al. [12] considered MHD two dimensional unsteady flow of a Newtonian fluid in a porous medium in the presence of heat generation and chemical reaction. Khalil-Ur-Rehman and Malik [13] examined mixed convection flow of Eyring-Powell fluid past a stretching cylindrical surface with heat generation/absorption effects. Adegbie and Fagbade [14] presented the problem of convective heat transfer flow of viscous fluid in the presence of thermal rediation and explored the qualitative properties of solution of ordinary differential equations arising from such flow model. Samuel and Ajayi [15] performed a numerical study of the radiation effect on buoyancy driven flow of non-Newtonian power law fluid past a catalytic surface. Oyelami and Dada [16] discussed free convection flow of Eyring-Powell radiating fluid in a porous medium under the influence of magnetic field and viscous dissipation. Ali et al. [17] utilized Galerkin weighted residual finite-element technique to analyze problems of heat transfer flow of nanofluid in the presence of natural convection. Zaidi and Ahmad [18] studied the effects of heat generation on buoyancy driven flow of viscous fluid through an inclined microchannel with slip conditions. Adegbie et al. [19] analytically examined the impacts of pertinent fluid parameters on free convective flow of Newtonian fluid past a continuous moving surface. Recently, Khan et al. [20] investigated heat generation and natural convection effects on incompressible nanofluids along a sphere in the presence of Brownian motion and thermophoresis. Anwar et al. [21] investigated MHD free convective flow of an optically thick Casson fluid in the presence of heat generation. Oyelami et al. [22] presented numerical solutions of chemical reaction parameter and radiation parameter effects on natural convection MHD flow on non-Newtonian fluid between porous plates.

Having reviewed the literature above, it is obvious that none of the authors studied the numerical solutions of flow model arising from MHD flow of chemically reactive radiating fluid with Joule heating and variable viscosity past a continuous moving plate, which is the objective of the present investigation. The strongly coupled nonlinear system of partial differential equations is transformed into system of ordinary differential equations using suitable transformations and then numerically solved via fourth order Runge-Kutta Fehlberg method and shooting technique. The behavior of fluid velocity, temperature and concentration under the influence of pertinent parameters are demonstrated via table and graphically.

2 Mathematical Formulation

A two-dimensional laminar free convection and heat transfer flow of an electrically conducting incompressible viscous fluid past a stretching surface is examined. The fluid viscosity is assumed to vary exponentially with temperature. Also, radiation effect is incorporated into heat equation. Furthermore, chemical reaction and Joule heating effects are incorporated. It is assumed that plate wall is heated by temperature T_f and concentration C_s. T_∞ and C_∞ denote free stream temperature and free stream concentration, respectively. The stretching velocity is expressed as $u_w(x) = bx$ where b is a positive constant. With the aforementioned assumptions coupled with Boussinesq approximations, the governing equations are

$$\frac{\partial u}{\partial x} + \frac{\partial v}{\partial y} = 0, \tag{1}$$

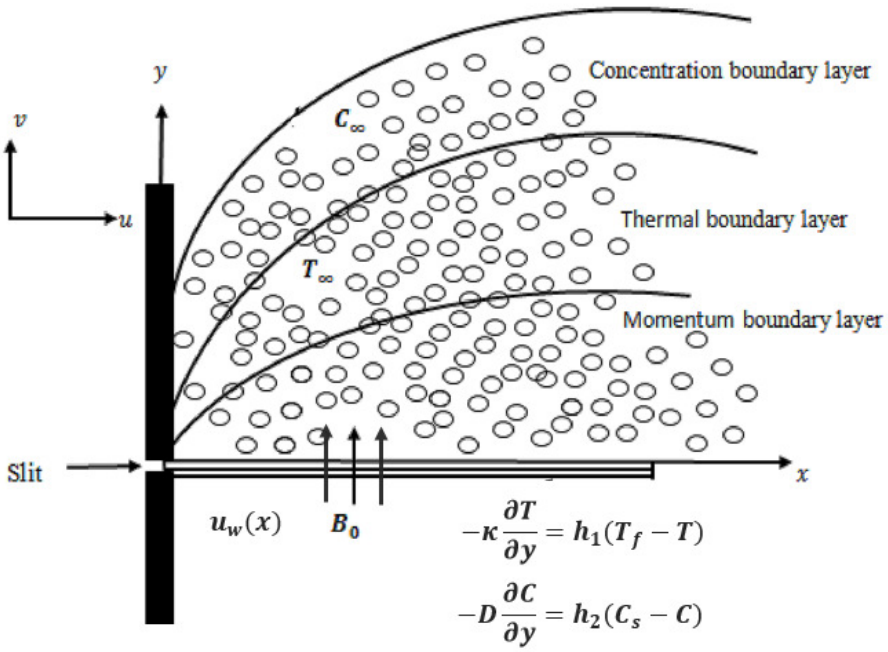

Figure 1: Schematic illustration.

$$u\frac{\partial u}{\partial x} + v\frac{\partial u}{\partial y} = \frac{1}{\rho_\infty}\frac{\partial}{\partial y}\left(\mu(T)\frac{\partial u}{\partial y}\right) - \frac{\sigma B_0^2}{\rho_\infty}u - \frac{\nu_\infty}{K'}u, \tag{2}$$

$$u\frac{\partial T}{\partial x} + v\frac{\partial T}{\partial y} = \frac{\kappa}{\rho_\infty c_p}\frac{\partial^2 T}{\partial y^2} - \frac{1}{\rho_\infty c_p}\frac{\partial q_r}{\partial y} + \frac{\sigma B_0^2}{\rho_\infty c_p}u^2, \tag{3}$$

$$u\frac{\partial C}{\partial x} + v\frac{\partial C}{\partial y} = D\frac{\partial^2 C}{\partial y^2} + \frac{Dk_T}{T_M}\frac{\partial^2 T}{\partial T^2} - K_c^*(C - C_\infty), \tag{4}$$

subject to the following boundary conditions

$$y = 0: \ u = u_w(x) = bx, \ v = 0, \ -\kappa\frac{\partial T}{\partial y} = h_1(T_f - T), \ -D\frac{\partial C}{\partial y} = h_2(C_s - C), \tag{5}$$

$$y \to \infty: \ u \to 0, \ T \to T_\infty, \ C \to C_\infty, \tag{6}$$

where B_o denotes magnetic field strength, u represents velocity component along x direction, v is the velocity component along y direction, ρ_∞ is the density of the fluid, μ_∞ is the fluid dynamic viscosity, κ is the fluid thermal conductivity, ν_∞ is the kinematic viscosity, σ denotes fluid electrical conductivity, c_p is the fluid specific heat at constant pressure, u_w is velocity with which the plate is moving, K_c^* is the rate of chemical reaction and D signifies mass diffusivity. q_r represents radiative heat flux which based on Rosseland approximation [21] is expressed as

$$q_r = -\frac{4\sigma^*}{3\kappa^*}\frac{\partial T^4}{\partial y}, \tag{7}$$

where σ^* is the Stefan-Boltzman constant and κ^* is the mean absorption coefficient. Further simplification of Eq. (7) gives

$$\frac{\partial q_r}{\partial y} = -\frac{4\sigma^*}{3\kappa^*}\frac{\partial^2 T^4}{\partial y^2} \approx -\frac{16\sigma^* {T_\infty}^3}{3\kappa^*}\frac{\partial^2 T}{\partial y^2}. \tag{8}$$

Also, the fluid viscosity is assumed to be a function of temperature and it is expressed as

$$\mu(T) = \mu_\infty e^{-\alpha(T-T_\infty)}, \tag{9}$$

where α is a constant.

By introducing the following similarity transformations in equations (1)-(3),

$$\eta = \left(\frac{b}{\nu_\infty}\right)^{\frac{1}{2}} y,\ u = bxf',\ v = -(\nu_\infty b)^{\frac{1}{2}} f,\ \theta = \frac{T-T_\infty}{T_f-T_\infty},\ \phi = \frac{C-C_\infty}{C_s-C_\infty}, \tag{10}$$

we obtain the following dimensionless equations,

$$f''' - \lambda f''\theta' + e^{\lambda\theta}\left[ff'' - (f')^2 - Mf' - K_p f'\right] = 0, \tag{11}$$

$$\left(1+\frac{4}{3}R_a\right)\theta'' + P_r[\theta' f + ME_c(f')^2] = 0, \tag{12}$$

$$\phi'' + S_c[\phi' f + S_r\theta'' - K_c\phi]. \tag{13}$$

the transformed boundary conditions are

$$f(0) = 0,\ f'(0) = 1,\ \theta'(0) = -Bi_1(1-\theta(0)),\ \phi'(0) = -Bi_2(1-\phi(0)), \tag{14}$$

$$f'(\infty) \to 0,\quad \theta(\infty) \to 0,\quad \phi(\infty) \to 0, \tag{15}$$

where $R_a = \frac{4\sigma^* T_\infty^3}{\kappa^* k_\infty}$ is the radiation parameter, $P_r = \frac{\mu_\infty c_p}{k_\infty}$ is the Prandtl number, $M = \frac{\sigma {B_0}^2}{\rho_b}$ is the magnetic parameter, $\lambda = \alpha(T_f - T_\infty)$ is the variable viscosity parameter, $K_p = \frac{\nu_\infty}{K' b}$ denotes porosity parameter, $E_c = \frac{u_w^2}{c_p(T_f-T_\infty)}$ represents Eckert number, $K_c = \frac{K_c^*}{b}$ represents chemical reaction parameter, $S_c = \frac{\nu_\infty}{D}$ is the Schmidt number, $S_r = \frac{Dk_T(T_f-T_\infty)}{\nu_\infty T_M(C_f-C_\infty)}$, $Bi_1 = \frac{h_1}{\kappa}(\frac{\nu_\infty}{b})^{\frac{1}{2}}$ represents Biot number, and $Bi_2 = \frac{h_2}{D_1}(\frac{\nu_\infty}{b})^{\frac{1}{2}}$ represents convective-diffusion parameter.

3 Numerical Computations

The system of non-linear ordinary differential Eqs. (11)-(13) subject to the boundary conditions (14)-(15) is solved numerically in the symbolic computation software MATLAB using Runge-Kutta fourth order scheme and shooting technique. The highly nonlinear coupled system of ODE in Eqs. (11)-(13) is reduced to a system of first order differential equations as follows: where,

$$\begin{aligned}
f_1' &= f_2,\\
f_2' &= f_3,\\
f_3' &= \lambda f_3 f_5 - e^{\lambda f_4}\left[f_1 f_3 - Mf_2 - (f_2)^2 - K_p f_2\right],\\
f_4' &= f_5,\\
f_5' &= (1/(1+(4/3)R_a))(-P_r(f_5 f_1 + ME_c(f')^2)),\\
f_6' &= f_7,\\
f_7' &= -S_c\Bigg[f_7 f_1 + S_r\Bigg(\Bigg(\Bigg(1/\left(1+\left(\frac{4}{3}\right)R_a\right)\Bigg)(-P_r(f_5 f_1 + \\
&\qquad ME_c(f')^2))\Bigg) - K_c f_6\Bigg].
\end{aligned} \tag{16}$$

Table 1: Comparison of skin friction coefficient for different values of M when $P_r = 1.0$, $E_c = \lambda = R_a = S_c = Bi_1 = Bi_2 = K_p = S_r = K_c = 0$.

M	Hayat et al. [23]	Mabood et al. [24]	Present study
0	-1.00000	-1.00000	-1.0005
1	-1.41421	-1.41421	-1.4142
5	-2.44948	-2.44949	-2.4495
10	-3.31662	-3.31662	-3.3166
50	-7.14142	-7.14143	-7.1414
100	-10.04987	-10.04987	-10.050

with the initial conditions

$$\begin{aligned} f_1(0) = 0,\ f_2(0) = 1,\quad f_3(0) = b_1, \\ f_4(0) = b_2,\ f_5(0) = -Bi_1(1 - f_4(0)), \\ f_6(0) = b_3,\ f_7(0) = -Bi_2(1 - f_6(0)), \end{aligned} \tag{17}$$

where guessed values are assigned to the unknown initial conditions b_1, b_2 and b_3. The resulting initial value problem is then solved numerically using a fourth order Runge Kutta-Fehlberg integration scheme and shooting technique.

4 Numerical Computations

In this section, the behaviour of flow field, fluid temperature and concentration profile under the effects of fluid parameters is discussed as shown in Figures 2-14 and table 1. Numerical computations are carried out taking into account the following values of parameters M =1.0, E_c= 0.5, $\lambda = 0.2$, R_a =0.5, $S_c = 0.7$, $Bi_1 = 1.0$, $Bi_2 = 1.0$, $P_r = 7.0$, $K_p = 1.0$, $S_r = 0.1$, $K_c = 1.0$. Table 1 presents comparison of the present result with the existing solutions in literature and excellent agreement is seen.

The effects of magnetic parameter M on velocity distributions are shown in Figures 2 and 3. Plot 2 presents a downtrend of the fluid velocity as magnetic parameter increases. This is due to the presence of Lorenz force which retards fluid flow. Also, Figure 3 demonstrates a surge in the fluid temperature for growing values of magnetic parameter M. Figure 4 represents the effect of various values of Biot number Bi_1 on temperature profile. The figure showed that fluid temperature increases with the increasing values of Bi_1. The variation of concentration profile for diverse values of convective-diffusion parameter Bi_2 is demonstrated in Figure 5. It is also noticed from this plot that energy level increases as Bi_2 increases.

Figure 6 illustrates the impact of Eckert number E_c on the temperature profile. It is observed that temperature profile is enhanced by large values of E_c. Figures 7 and 8 show the effect of different values of porosity parameter K_p on velocity profile and temperature profile. Figure 7 depicts that the fluid velocity decreases for higher values of K_p. But from Figure 8, it is observed that the temperature distributions increase for large values of K_p. The influence of radiation parameter R_a on the temperature profile is represented in Figure 9. From the plot, it is noticed that temperature profile enhances as values of R_a increases.

Figure 10 indicates the effect of different values chemical reaction parameter K_c on concentration profile. It reveals that the concentration distribution decreases as the values of K_c grow. The effect of variable viscosity parameter λ on velocity distribution is presented in Figure 11.

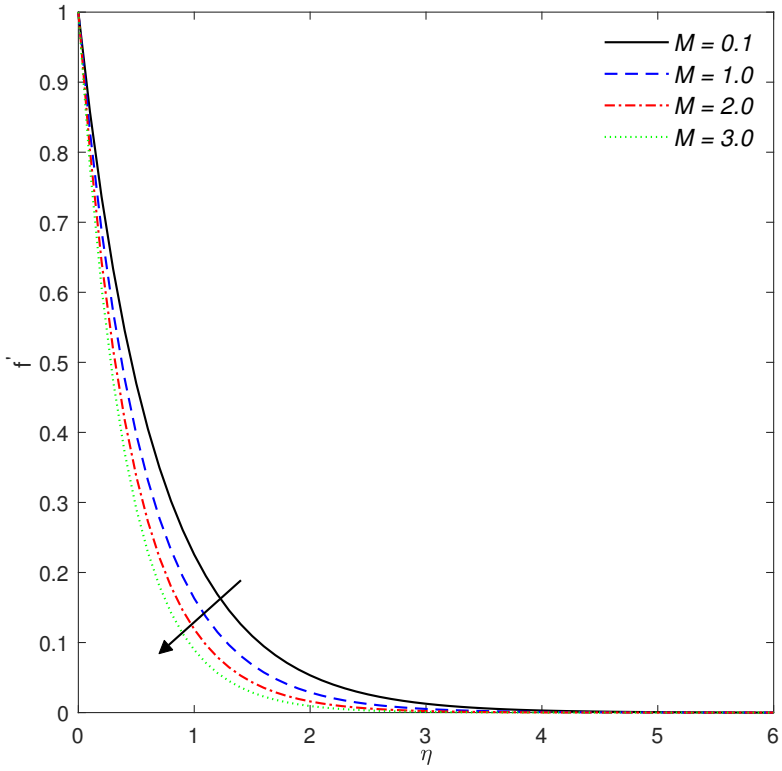

Figure 2: Velocity profile for various values of M.

It is observed that an increase in the values of λ weakens the fluid flow. This is expected as large values of variable viscosity parameter λ imply that the fluid is highly viscous. Figure 12 shows the behaviour of temperature distribution under the impact of Prandtl number P_r. The plot shows that fluids with higher values of Pr have lower temperature.

Figure 13 exhibits the influence of Soret number S_r on concentration profile. The graph shows that a rise in S_r escalates the concentration distribution. Figure 14 presents the behaviour of concentration profile for distinct values of Schmidt number S_c. It is noticed from the figure that concentration profile shows decreasing behavior as S_c increases.

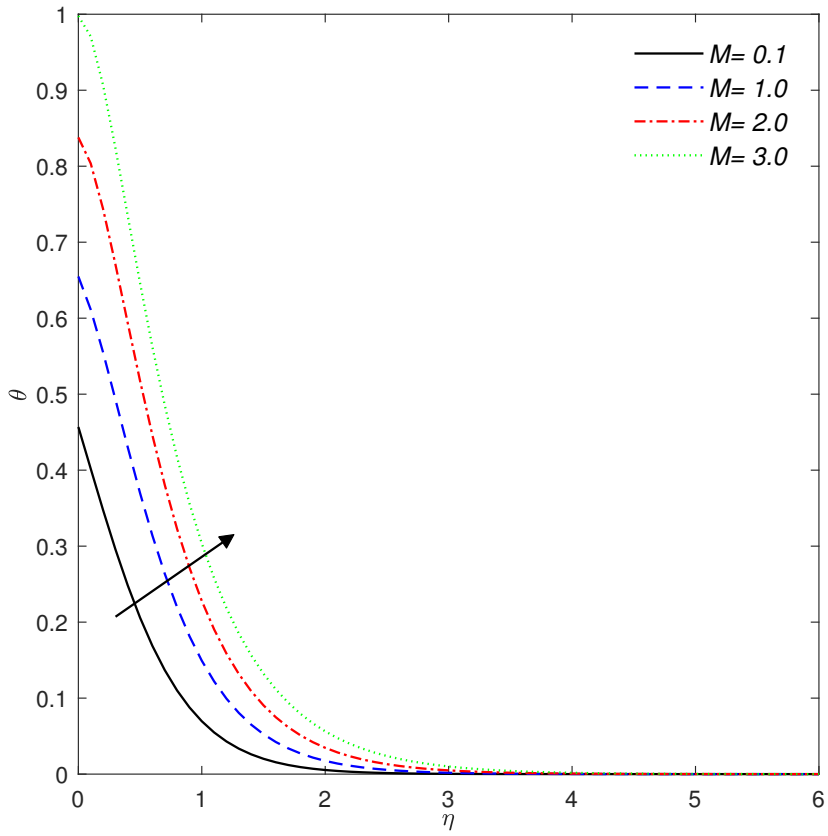

Figure 3: Temperature profile for various values of M.

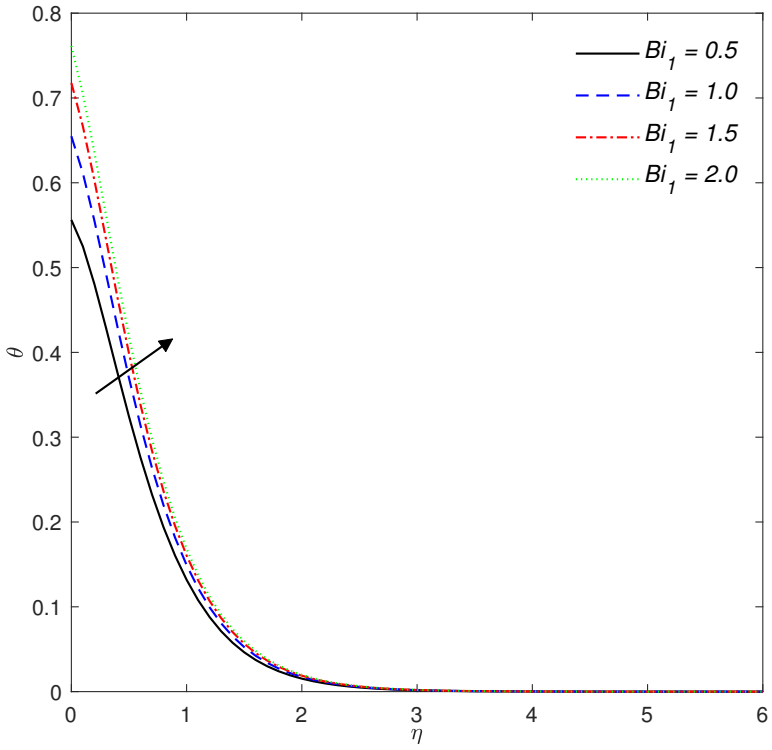

Figure 4: Temperature profile for various values of Bi_1.

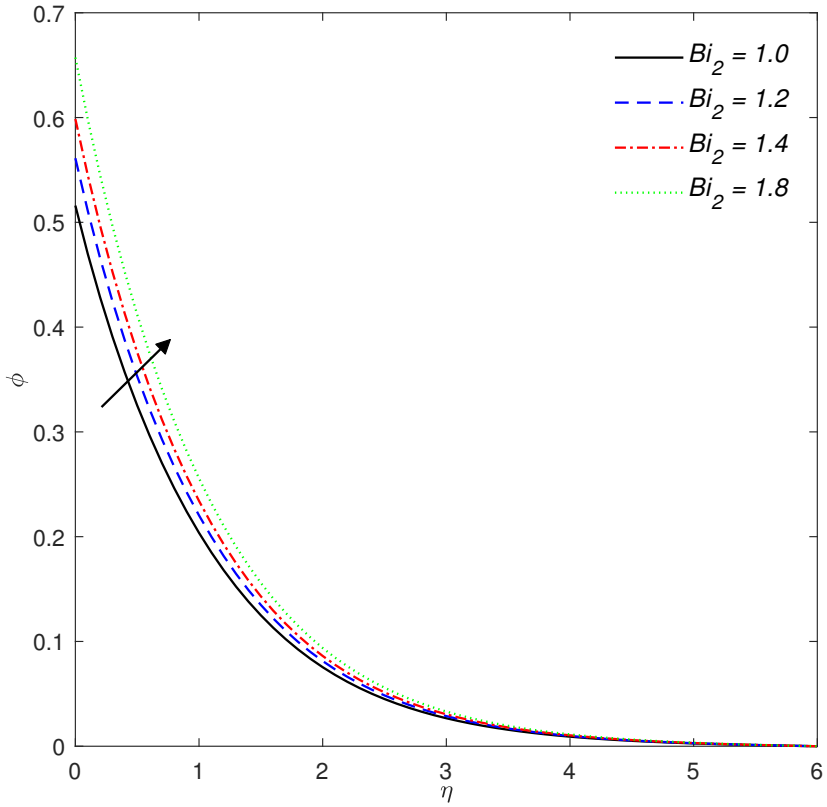

Figure 5: Concentration profile for various values of Bi_2.

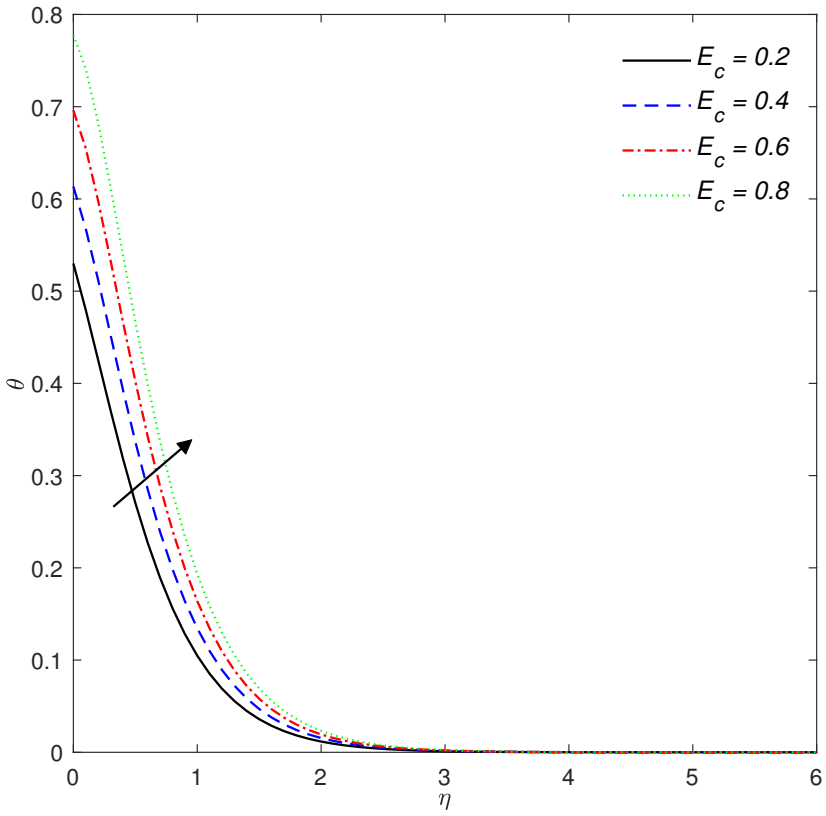

Figure 6: Temperature profile for various values of E_c.

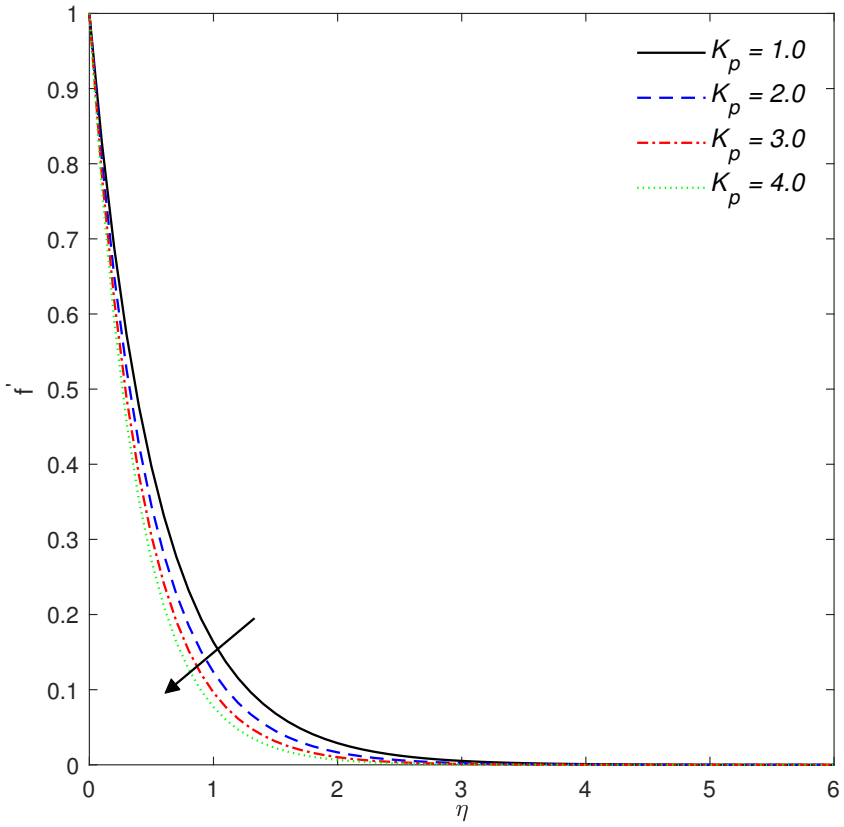

Figure 7: Velocity profile for various values of K_p.

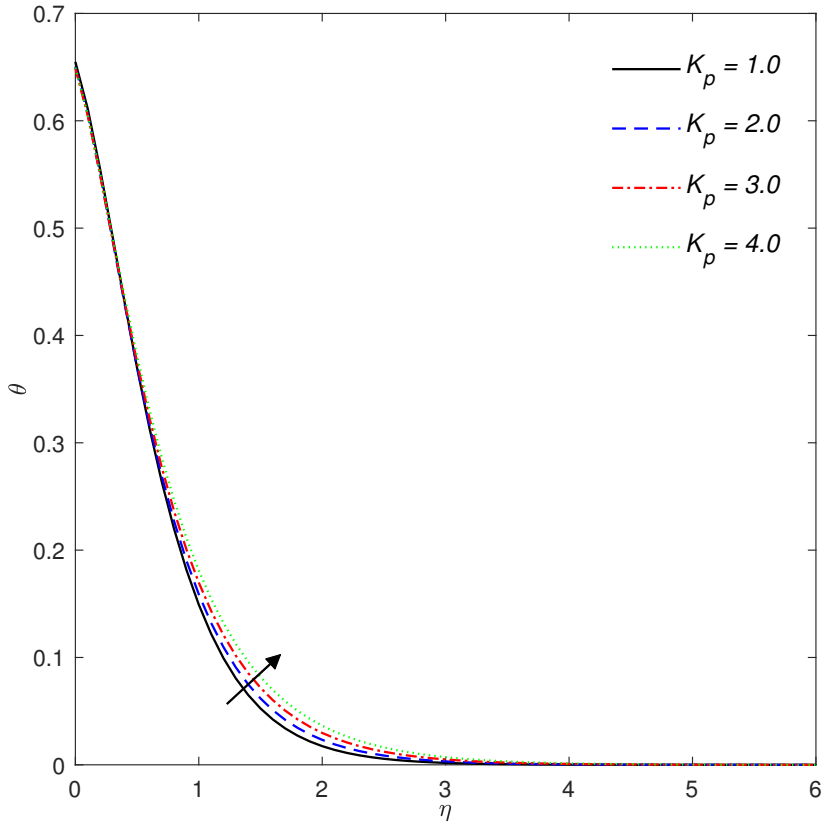

Figure 8: Temperature profile for various values of K_p.

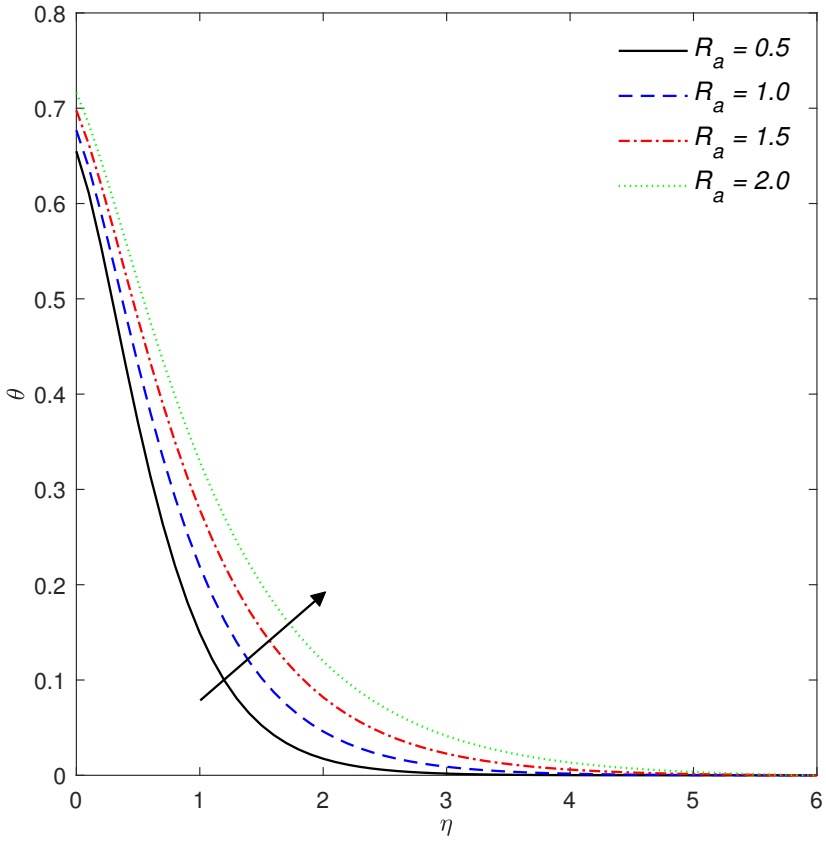

Figure 9: Temperature profile for various values of R_a.

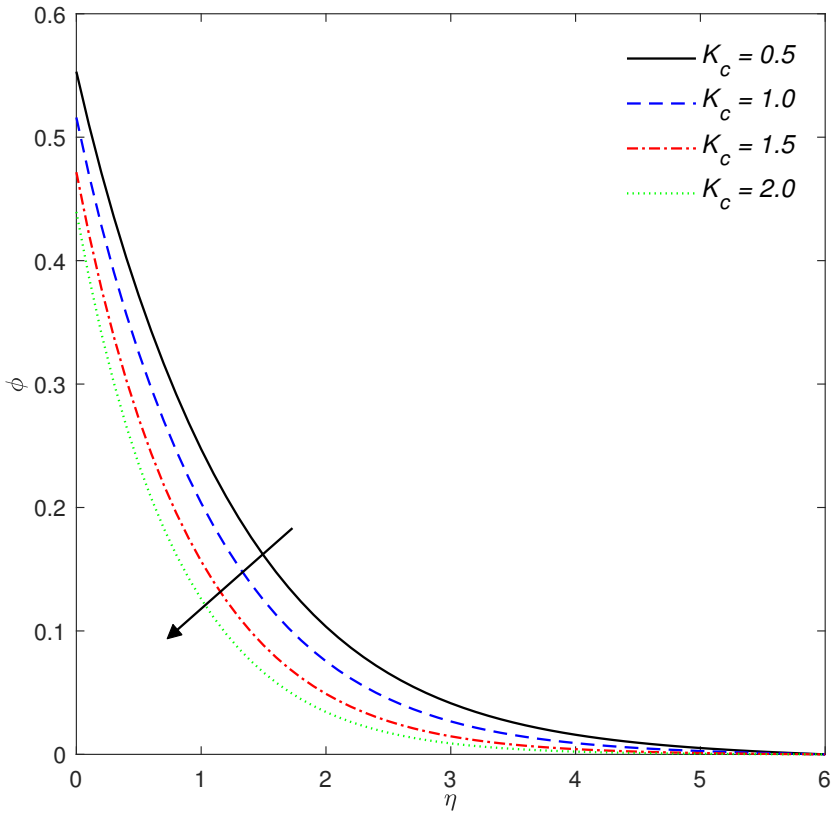

Figure 10: Concentration profile for various values of K_c.

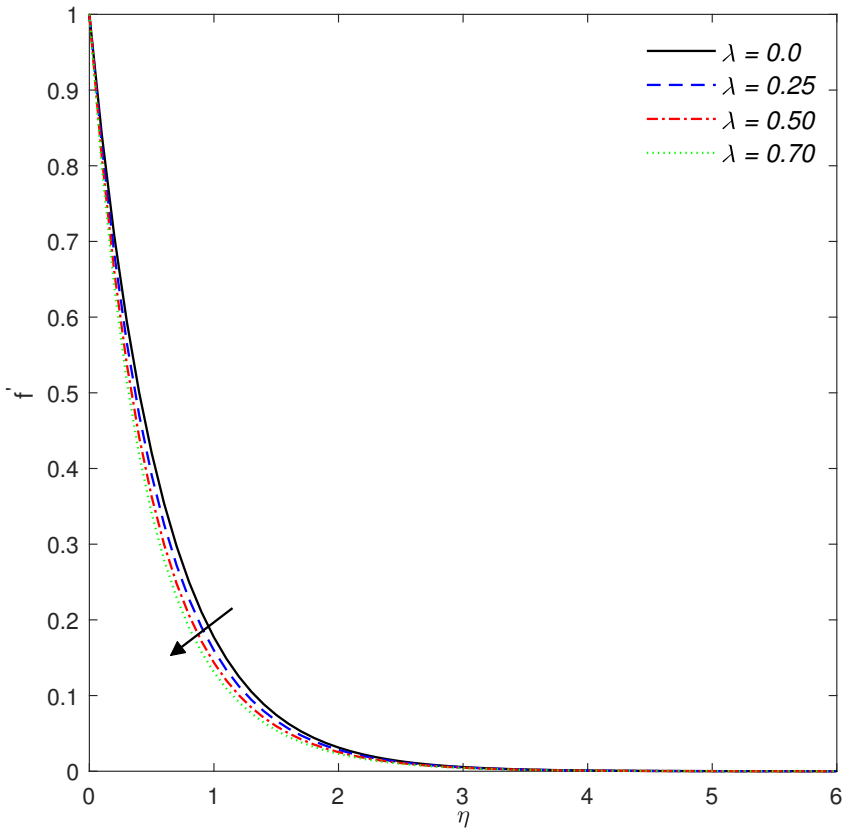

Figure 11: Velocity profile for various values of λ.

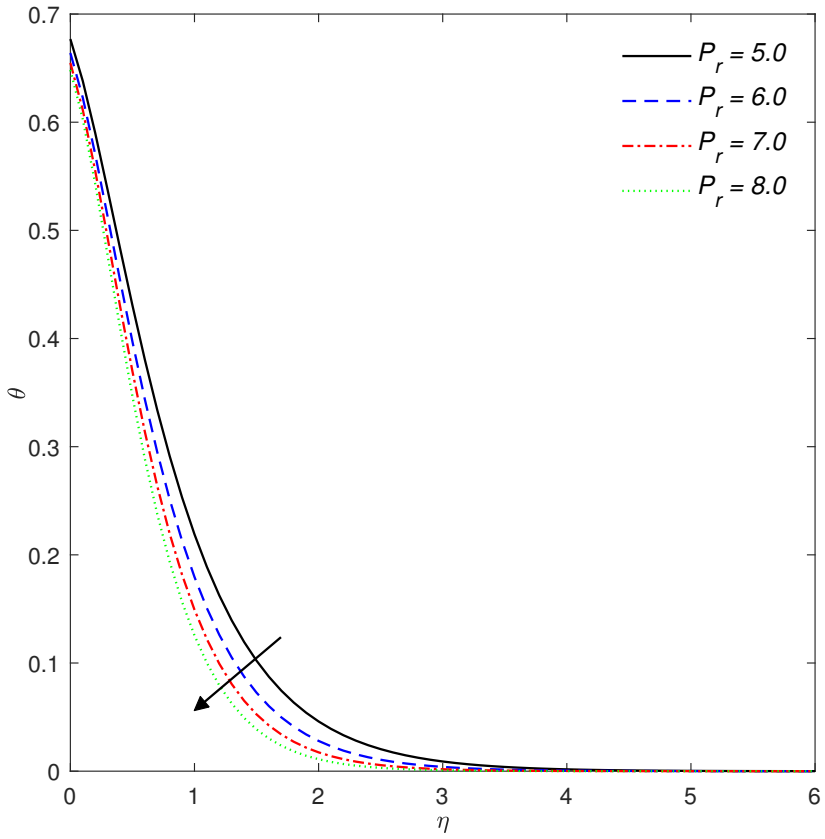

Figure 12: Temperature profile for various values of P_r.

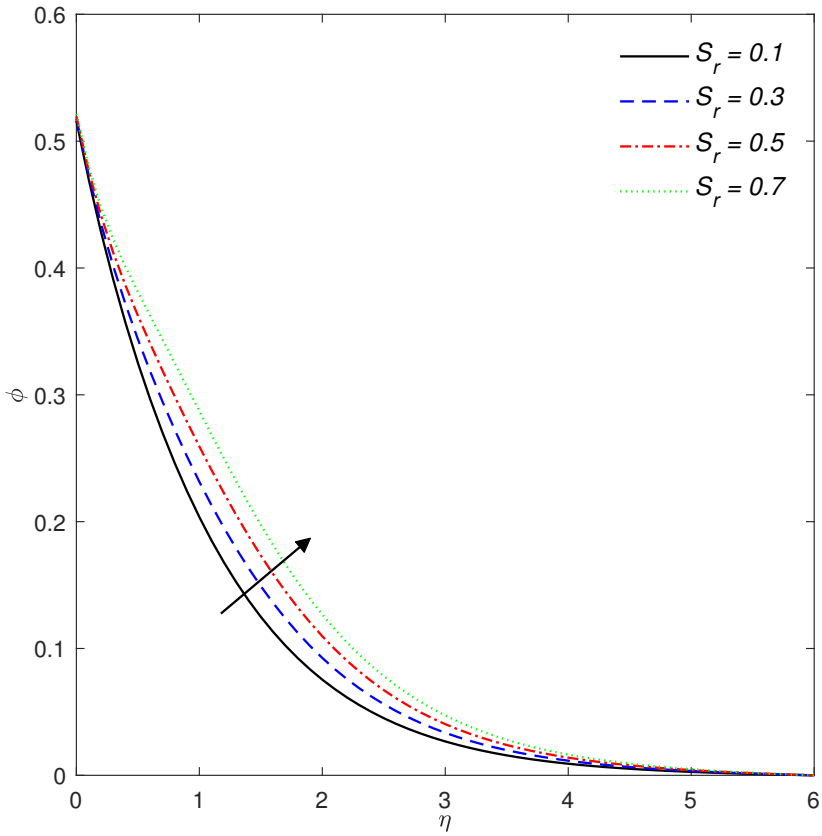

Figure 13: Concentration profile for various values of S_r.

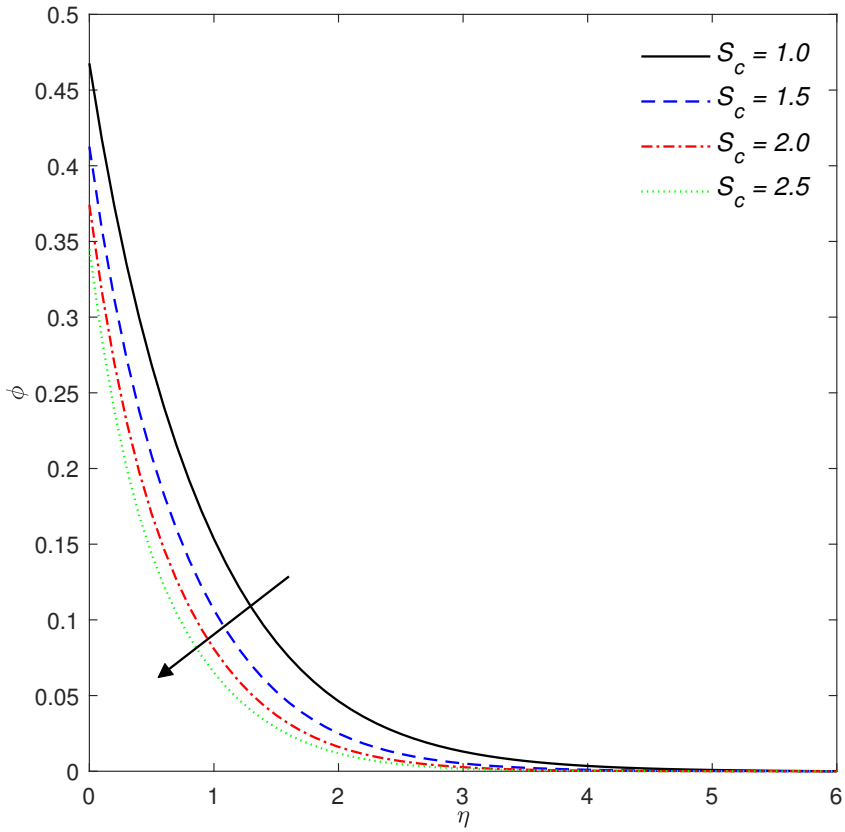

Figure 14: Concentration profile for various values of S_c.

5 Conclusion

Heat and mass transfer impact on steady flow of chemically reacting radiating fluid in a porous medium subject to magnetic field and Joule heating is investigated. The behaviors of velocity, temperature and concentration profiles for different values of flow parameters are discussed through graphs and tables. The transformed system of strongly coupled nonlinear ordinary differential equations is solved numerically using Runge-Kutta Fehlberg method. Remarkable findings from the present study are as follows:

1. the velocity profiles are depreciated for larger values of variable viscosity parameter and porosity parameter;

2. the fluid temperature is raised in the presence of Biot number, radiation parameter and Eckert number; and

3. growing values of chemical reaction parameter and Schmidt number significantly weaken the concentration distribution.

References

[1] Ryoichi, A., Fueki, K., and Mukaibo, T. (1975). Application of magnetohydrodynamic effect to the analysis of electrochemical reactions 1. MHD flow of an electrolyte solution in an electrode-cell with a short rectangular channel. Denki Kagaku Oyobi Kogyo Butsuri Kagaku, 43(9), 504-508.

[2] Pakmor, R., Bauer, A., and Springel, V. (2011). Magnetohydrodynamics on an unstructured moving grid. Monthly Notices of the Royal Astronomical Society, 418(2), 1392-1401.

[3] Opanuga, A. A., Gbadeyan, J. A., and Iyase, S. A . (2017). Second law analysis of a reactive MHD couple stress fluid through porous medium. International Journal of Applied Mathematics and Statistics, 56(5).

[4] Gedik, E., Kurt, H., and Recebli, Z. (2013). CFD simulation of magnetohydrodynamic flow of a liquid-metal Galinstan fluid in circular pipes. FDMP-Fluid Dynamics and Materials Processing, 9(1), 23-33.

[5] Azimi-Boulali, J., Zakeri, M., and Shoaran, M. (2019). A study on the 3D fluid flow of MHD micropump. Journal of the Brazilian Society of Mechanical Sciences and Engineering, 41, 478.

[6] Zaman, H., Ahmad, Z., and Ayub, M. (2013). A note on the unsteady incompressible MHD fluid flow with slip conditions and porous walls. International Scholarly Research Notices, 2013, Article ID 705296, 10 pages.

[7] Rao, M. V. S., Gangadhar, K., and Varma, P. (2018). A spectral relaxation method for three-dimensional MHD flow of nanofluid flow over an exponentially stretching sheet due to convective heating: an application to solar energy. Indian Journal of Physics, 92, 1577-1588.

[8] Mandal, H. K., Das, S., and Jana, R. N. (2014). Transient free convection in a vertical channel with variable temperature and mass difussion. International Institute for Science Technology and Education, 23,

[9] Miroshnichenko, I. V., and Sheremet, M. A. (2015). Numerical simulation of turbulent natural convection combined with surface thermal radiation in a square cavity. International Journal of Numerical Methods for Heat and Fluid Flow, 25(7), 1600-1618.

[10] Samuel, D. J. (2018). Chemical reaction and melting heat effects on MHD free convective radiative fluid flow past a continuous moving plate in the presence of thermo-physical parameters. Defect and Diffusion Forum, 384, 80-98.

[11] Saravanan, S., and Chinnasamy, S. (2015). Combined natural convection and thermal radiation in a square cavity with a non-uniformly heated plate. Computers and Fluids, 117, 125-138.

[12] Satya, S., Saxena, and Dubey, G. (2011). Unsteady MHD heat and mass transfer free convection flow of polar fluids past a vertical moving porous plate in a porous medium with heat generation and thermal diffusion. Advances in Applied Science Research, 2(4), 259-278.

[13] Khalil-Ur-Rehman, and Malik, M. Y. (2017). Application of shooting method on MHD thermally stratified mixed convection flow of non-Newtonian fluid over an inclined stretching cylinder. Journal of Physics: Conference Series, 822, 012012.

[14] Adegbie, K. S., and Fagbade, A. (2015). A note on qualitative properties of solution to a system of differential equations arising from Magnetohydrodynamic fluid flow in a saturated porous medium. Journal of Nigerian Association of Mathematical Physics, 29, 95-110.

[15] Damilare John Samuel, Babatunde Oluwaseun Ajayi. (2018). The effects of thermo-physical parameters on free convective flow of a chemically reactive power law fluid driven by exothermal plate. Chemical and Biomolecular Engineering, 3(3), 22-34.

[16] Oyelami, F. H., and Dada, M. S. (2018). Unsteady magnetohydrodynamic flow of some non-Newtonian fluids with slip through porous channel, International Journal of Heat and Technology, 36(2), 709-713.

[17] Ali M. M., Alim M. A., Akhter R., and Ahmed S. S. (2017). MHD natural convection flow of CuO/Water nanofluid in a differentially heated hexagonal enclosure with a tilted square block. International Journal of Applied and Computational Mathematics, 3, 1047-1069.

[18] Hasan Nihal Zaidi, Naseem Ahmad, (2017). MHD convection fluid flow and heat transfer in an inclined microchannel with heat generation. American Journal of Applied Mathematics, 5(5), 124-131.

[19] Adegbie, K. S., Samuel, D. J., and Ajayi, B. O. (2019). Ohmic heating of magnetohydrodynamic viscous flow over a continuous moving plate with viscous dissipation buoyancy and thermal radiation. Defect and Diffusion Forum, 392, 73-91.

[20] Khan, A., Ashraf, M., Rashad, A., and Nabwey, H. (2020). Impact of heat generation on magneto-nanofluid free convection flow about sphere in the plume region. Mathematics, 8(11), 2010.

[21] Anwar, T., Kumam, P., and Watthayu, W. (2021). Unsteady MHD natural convection flow of Casson fluid incorporating thermal radiative flux and heat injection/suction mechanism under variable wall conditions. Scientific Reports, 11, 4275.

[22] Oyelami, F. H., Ige, E. O., Saka-Balogun, O. Y., and Adeyemo, O. A. (2021). Study of heat and mass transfer to magnetohydrodynamic (MHD) pulsatile couple stress fluid between two parallel porous plates. Instrumentation Mesure Métrologie, 20(4), 179-185.

[23] Hayat,T., Hussain, Q., and Javed, T. (2009). The modified decomposition method and Padé approximants for the MHD flow over a non-linear stretching sheet. Nonlinear Analysis: Real World Applications, 10(2), 966?973.

[24] Mabood, F., Bognár, G., and Shafiq, A. (2020). Impact of heat generation/absorption of magnetohydrodynamics Oldroyd-B fluid impinging on an inclined stretching sheet with radiation. Scientific Reports, 10, 17688.